ACS APPLIED MATERIALS & INTERFACES

www.acsami.org

Forum Article

Rational Control of the Activity of a Cu^{2+}-Dependent DNAzyme by Re-engineering Purely Entropic Intrinsically Disordered Domains

Daniela Sorrentino, Simona Ranallo, and Francesco Ricci*

Cite This: https://dx.doi.org/10.1021/acsami.0c09472

Read Online

ACCESS | Metrics & More | Article Recommendations | Supporting Information

ABSTRACT: The function and activity of many proteins is finely controlled by the modulation of the entropic contribution of intrinsically disordered domains that are not directly involved in any recognition event. Inspired by this mechanism, we demonstrate here that we could finely regulate the catalytic activity of a model DNAzyme (i.e., a synthetic DNA sequence with enzyme-like properties) by rationally introducing intrinsically disordered nucleic acid portions in its original sequence. More specifically, we have re-engineered here the well-characterized Cu^{2+}-dependent DNAzyme that catalyzes a self-cleavage reaction by introducing a poly(T) linker domain in its sequence. The linker is not directly involved in the recognition event and connects the two domains that fold to form the catalytic core. We demonstrate that the enzyme-like activity of this re-engineered DNAzyme can be modulated in a predictable and fine way by changing the length, and thus entropy, of such a linker domain. Given these attributes, the rational design of intrinsically disordered domains could expand the available toolbox to achieve a control of the activity of DNAzymes and, in analogy, ribozymes through a purely entropic contribution.

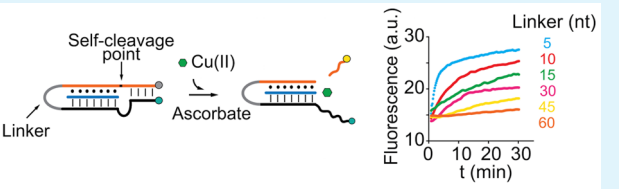

KEYWORDS: *DNA nanotechnology, DNAzyme, intrinsic disorder, entropy, ribozymes*

INTRODUCTION

DNAzymes and ribozymes are nucleic acid strands able to catalyze specific chemical reactions with enzyme-like efficiency and selectivity.[1] While ribozymes are naturally occurring RNA-based sequences that were first observed more than 30 years ago,[2−4] their DNA-based counterparts (i.e., DNAzymes) were selected in vitro for the first time in 1994 by Joyce and Breaker, who isolated a DNA sequence able to catalyze the cleavage of a phosphodiester bond in the presence of Pb^{2+} ions.[5] After this first example, many DNAzymes with specific catalytic activities have been described: phosphorylation,[6] ligation,[7] deglycosylation,[8] and metal-dependent hydrolytic cleavage of DNA substrates[9−18] as well as reactions involving non-nucleic-acid substrates,[19] have been reported to date.[20,21]

The most appealing feature of catalytic nucleic acids is the fact that they couple the positive features of enzymes (e.g., catalytic activity and specificity) with those of synthetic nucleic acids (e.g., programmability and low cost). In particular, the predictable nature of DNA−DNA interactions compared to those (amino-acid-based) much more complex involved in enzyme folding and function makes possible to control DNAzymes' activity in a rational way with different strategies. For example, DNAzymes have been rationally re-engineered with an allosteric domain to control the catalytic activity with different effectors (short oligonucleotide sequences,[22−27] small molecules,[28−30] and peptides or proteins).[31,32] Similarly, pH-programmable DNAzymes have been proposed by Willner and co-workers and other groups introducing *i*-motif regions in the nucleic acid sequence.[33−35] The above approaches underline the ease with which DNAzymes can be controlled. However, they are not without limitations: they in fact require careful design and modification of the DNAzyme sequence and often need several trial and error attempts. It would thus be important to find new strategies to rationally control the activity of DNAzymes and overcome the above limitations.

Many proteins and enzymes contain intrinsically disordered domains that, although not directly involved in the recognition event, influence their folding process and thus their functional activity. Changes in the disorder associated with these domains allow through a purely entropic contribution the activity of these bioreceptors to be controlled in a highly precise way.[36−41] A similar mechanism also allows the response behavior of DNA-based synthetic receptors to be modulated[42,43] and could thus be recreated in enzyme-like synthetic devices (i.e., DNAzymes) as a novel and versatile way to control their catalytic activity.

Special Issue: Materials Applications of Aptamers

Received: May 24, 2020
Accepted: September 11, 2020

EXPERIMENTAL SECTION

Chemicals. All reagent-grade chemicals, including NaCl, EDTA ($(HO_2CCH_2)_2NCH_2CH_2N(CH_2\ CO_2H)_2$), (+)-sodium L-ascorbate ($C_6H_7NaO_6$), HEPES sodium salt ($C_8H_{17}N_2NaO_4S$), $Cu(NO_3)_2$, $MgCl_2$, $Pb(NO_3)_2$, $FeCl_3$, acrylamide-bis-acrylamide (40%), ammonium persulfate ($(NH_4)_2S_2O_8$), urea, Trizma base, tetramethylethylenediamine ($(CH_3)_2NCH_2CH_2N(CH_3)_2$) and boric acid ($H_3BO_3$) from Sigma-Aldrich, St. Louis, Missouri, were used as received. O'RangeRuler 50bp DNA Ladder and SYBR gold were purchased from ThermoFisher Scientific (USA).

Oligonucleotides. HPLC purified oligonucleotides were purchased from IBA (Gottingen, Germany) or Biosearch Technologies (Risskov, Denmark). The different DNAzyme variants were modified with FAM (5-carboxyfluorescein), at the 3′ end, and BHQ-1 (black hole quencher 1), at the 5′ end. All oligonucleotides were dissolved in double distilled water (ddH_2O) at a concentration of 100 μM and aliquoted at −20 °C for long-term storage. All sequences for the DNAzyme variants were designed using Nupack.[44] All sequences are reported in the Supporting Information.

Fluorescent Experiments. Fluorescent experiments were performed at pH 6.5 in 0.15 M NaCl, 50 mM HEPES sodium salt, 30 nM EDTA, 50 μM (+)-sodium L-ascorbate in a 100 μL cuvette (total volume of the solution 100 μL). Equilibrium fluorescence measurements were obtained using a Cary Eclipse Fluorimeter (Agilent Technologies) respectively with excitation at 495 (±5) nm and acquisition at 517 (±10) nm. Binding curves of the DNAzyme variants were obtained by preparing a 100 μL solution containing 20 nM of DNAzyme and by sequentially increasing the concentration of the target DNA substrate. For each concentration, the fluorescence signal was recorded every 15 min until it reached equilibrium. For the binding curves, the observed fluorescence, $F_{[\text{DNA substrate}]}$, was fitted using the following four parameter logistic equation

$$F_{[\text{DNA substrate}]} = F_{\min} + (F_{\max} - F_{\min})[[\text{DNA substrate}]^{\text{nH}} / ([\text{DNA substrate}]^{\text{nH}} + K_{1/2}{}^{\text{nH}})]$$

where, $F_{\min}$ and $F_{\max}$ are the minimum and maximum fluorescence values, $K_{1/2}$ is the equilibrium target concentration at half-maximum signal, nH is the Hill coefficient, and [DNA substrate] is the concentration of the target added. This model is not necessarily physically relevant, but it does a good (empirical) job of fitting effectively bilinear binding curves such as those we obtain for most of our nanoswitches, providing a convenient and accurate means of estimating $K_{1/2}$. Data were normalized on a 0−1 scale to allow for more ready interpretation of the results.

Cu^{2+} Titration Curves. For all the DNAzyme variants titration curves obtained by adding increasing concentrations of Cu^{2+} ions were conducted at pH 6.5 in 0.15 M NaCl, 50 mM HEPES sodium salt, 30 nM EDTA, 50 μM (+)-Sodium L-ascorbate at 45 °C in a 100 μL cuvette (total volume of the solution 100 μL). Such kinetic experiments were performed by preparing a 100 μL solution containing 20 nM of DNAzyme, 300 nM of DNA substrate and by sequentially increasing the concentration of $Cu(NO_3)_2$.

Thermal Melting Curves. Fluorescence versus temperature profiles (thermal melting curves) were obtained by preparing a 100 μL solution containing 20 nM of DNAzyme and 5 μM of DNA substrate to saturate the nanoswitch and waiting 10 min before temperature ramping. Melting curves were conducted using a Cary Eclipse fluorimeter (Agilent Technologies) with an excitation wavelength at 495 (±5) nm and an acquisition wavelength at 517 (±10) nm. Melting curves were performed by heating from 15 to 95 °C at a rate of 1 °C·min^{-1} using a total reaction volume of 100 μL in a quartz cuvette. All the reported melting curves were normalized on a scale from 0.01 (set as background signal) to 1 through the use of the interpolation model that allows the melting temperature (T_m) to be estimated for each experiment. Two baselines (upper and lower) have been chosen as straight lines fitting the fluorescence signal before and after the melting transition. Such baselines correspond to the unfolded (random coil) and folded (triplex) states, respectively. Through the average of the estimated baselines, it is possible to calculate a median line. Such a median line will be drawn within the two baselines crossing the experimental curve in the melting transition region. The T_m corresponds to the crossing point between the experimental curve and the median line, and its uncertainty is estimated at ±0.5 °C. Please refer to the Supporting Information for the thermodynamic analysis of thermal melting curves.

Denaturing Urea/Polyacrylamide Gel Experiments. Denaturing UREA PAGE gels were prepared by adding urea to double distilled water (ddH2O) in a specific ratio to cast the desired polyacrylamide percentage (15%). The mixture was then heated until the urea completely dissolved. This mixture was allowed to cool to room temperature, and then, acrylamide/bis-acrylamide (40%) solution was added. Into this solution was then added TBE (10×), ammonium persulfate (APS), and tetramethylethylenediamine (TEMED) in appropriate ratios. Gels were cast in 10 × 10 cm, 1.5 mm thick disposable mini gel cassettes and allowed to polymerize for at least 30 min before electrophoresis. DNAzyme samples were obtained by preparing a 100 μL solution containing 100 nM of DNAzyme, 300 nM of target DNA substrate, and 3 μM of Cu^{2+} in 0.15 M NaCl, 50 mM HEPES sodium salt, 30 nM EDTA, and 50 μM (+)-sodium L-ascorbate at pH 6.5 at 45 °C. A volume of 10 μL of each sample was added into the gel for electrophoresis. Then, gels were run at room temperature at a constant voltage of 100 V for 1 h 30 min in TBE (1×) in a Bio-Rad PowerPac Basic power supply. After electrophoresis, the gels were stained in SYBR Gold Nucleic Acid Gel Stain for 20−30 min and imaged using the Gel Doc XR system (Bio-Rad).

RESULTS AND DISCUSSION

Motivated by the above considerations, here we propose to rationally design intrinsically disordered domains in the sequence of a DNAzyme to finely regulate its catalytic activity through a purely entropic contribution. To do this, we have re-engineered the widely used and well-characterized DNAzyme developed by Breaker and co-workers that displays a Cu^{2+}-induced self-cleavage activity.[11−14] The original Cu^{2+}−DNAzyme is composed of two DNA strands: one (black, Figure 1a) forms a unimolecular hairpin duplex and binds with the second strand (orange, Figure 1a) through duplex (Watson−Crick) and triplex (Hoogsteen) interactions to form the catalytic core. In the presence of Cu^{2+} ions and ascorbate, this bimolecular complex catalyzes the self-cleavage of one of the two strands (Figure 1a). To control the activity of this DNAzyme with intrinsically disordered regions, we have re-engineered the two strands so that the same catalytic core can be formed by a bimolecular binding event between a triplex-forming clamp-like strand (black and orange, Figure 1b) and a 11-nt substrate strand (blue strand, Figure 1b).

First, we demonstrate that the re-engineered DNAzyme maintains the same self-cleavage activity as the original DNAzyme. To do so, we have optically labeled the clamp-like triplex-forming DNA strand at the two ends so that an increase in fluorescence signal is observed as a result of the Cu^{2+}-triggered self-cleaving activity (Figure 1b). As expected, the clamp-like strand only shows self-cleavage activity in the presence of both Cu^{2+} ions and the substrate strand, demonstrating that the redesigned clamp-like strand can effectively form the bimolecular catalytic complex core in the presence of the specific DNA substrate (Figure 1c).

Because the formation of the bimolecular catalytic complex core is crucial for the cleavage activity of the DNAzyme, it is possible to rationally control the activity of the DNAzyme by modulating the affinity of the clamp-like strand for the substrate strand. To control the activity of such DNAzyme

https://dx.doi.org/10.1021/acsami.0c09472
ACS Appl. Mater. Interfaces XXXX, XXX, XXX−XXX

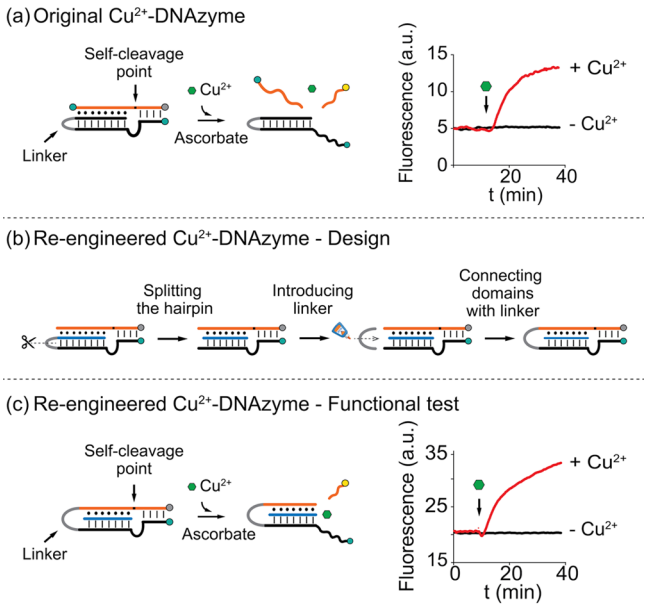

Figure 1. (a) Original Cu^{2+}-dependent DNAzyme composed of two DNA strands able to form a catalytic core that, in the presence of Cu^{2+} ions and ascorbate, catalyzes the cleavage of one of the two strands, resulting in an increase of the fluorescence signal. (b) Rational design of a re-engineered Cu^{2+}-dependent DNAzyme. We split the hairpin strand and introduced a linker strand to connect the two domains. The linker domain can be conveniently varied to control functionality of the DNAzyme. (c) The so re-engineered DNAzyme maintains the same catalytic activity as the original DNAzymes undergoing a self-cleavage of the clamp-like strand in the presence of Cu^{2+} ions and ascorbate. The experiments were performed in a pH 6.5 0.15 M NaCl, 50 mM HEPES, 30 nM EDTA, 50 μM ascorbate buffer (for this and the following figures) at 45 °C in the presence of 20 nM of the hairpin duplex and 10 nM of the substrate strand (orange) for the original DNAzyme (a) and in the presence of 20 nM of the clamp-like strand and 300 nM of the DNA substrate (blue) for the re-engineered DNAzyme (c). Cu^{2+} was added at a final concentration of 3 μM.

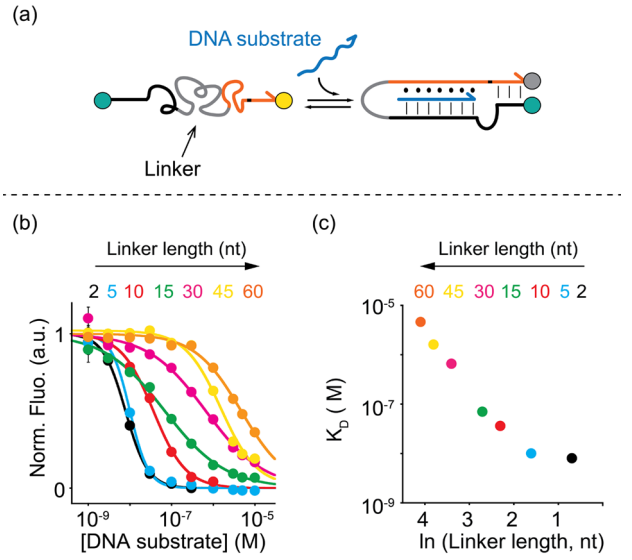

Figure 2. (a) Re-engineered DNAzyme forms the catalytic core (indicated) through binding between the triplex-forming strand and a single strand DNA substrate. (b) Binding curves obtained with a set of DNAzyme variants sharing the same triplex-forming recognition portion and varying lengths of the linker domain. (c) By tuning the length of the linker portion that connects the two binding domains, the observed affinity of the DNAzyme for its substrate can be precisely controlled. The titration experiments were performed at 35 °C in the presence of 20 nM of DNAzyme and adding increasing concentrations of the 11-nt DNA substrate. The experimental values represent averages of three separate measurements, and the error bars reflect the standard deviations in this and the following figures. For a matter of clarity in the binding curves, error bars have been depicted for only one point on each curve and represent the maximum value of standard deviation, and the arrow indicates the 3′ end (for this and the following figures).

with intrinsic disorder, we have thus designed a set of DNAzyme variants, in which we varied the length, and thus entropic contribution, of the poly(T) linker of the clamp-like triplex-forming strand (gray domain in Figure 2a) that connects the two recognition domains. For the design of the linker, poly(T) DNA sequences have been used, as they have been already demonstrated to behave as purely entropic domains,[36,37] and they were preferred over poly(A) and poly(C) sequences that, due to intramolecular base stacking and formation of secondary structures, could provide an additional enthalpic contribution. To first study the effect of the entropic cost associated with the different linkers on the binding affinity for the DNA substrate, we construct titration curves with the DNA substrate for all the variants in the absence of Cu^{2+} ions (Figure 2a,b). As expected, at increasing concentrations of the DNA substrate, we observe a decrease of the fluorescence signal associated with the triplex formation that brings the fluorophore and quencher closer. We observe a decrease of the affinity for the DNA substrate, as the length of the linker domain is increased (Figure 2b). More specifically, the dissociation constant (K_D) value for the binding of the DNA substrate changes from 8 ± 1 nM to 4 ± 1 μM upon increasing the length of the poly(T) linker from 2 to 60 nucleotides (nt), respectively (Figure 2c and Table S1).

To better understand how the linker length affects the binding affinity of the clamp-like strand for the DNA substrate, we have determined the entropic contribution of the different linker portions by constructing thermal melting curves (Figure 3a).[45] According to the linker-dependent modulation of the DNA substrate affinity, upon increasing the length of the poly(T) linker, we observe lower melting temperatures, as the entropy associated with the linker destabilizes the duplex DNA (Figure 3b and Tables S2 and Table S3). As expected, because the DNAzyme variants differ only in the length of the linker domain but share the same recognition portion, the enthalpic contribution of the binding event (given by the slope of the van't Hoff plots) is the same for all the different variants tested (Figure 3c, Figure S1, and Table S2). We can thus conclude that the observed difference in free energy values between DNAzymes with different linker lengths is due to the different entropic contribution associated with the different poly(T) linker portion. As expected in the case of a random coil polymer, the ΔS values calculated from van't Hoff analysis scale with the natural logarithm of the number of nucleotides in the linker (Figure S2).

To evaluate how the entropic cost associated with the linker domain affects the catalytic activity of the DNAzyme, we have tested all the variants in the presence of the DNA substrate and Cu^{2+} ions (Figure 4a). Specifically, by adding increasing concentrations of Cu^{2+} ions to a solution containing the clamp-forming strand and the DNA substrate, we can finely modulate the catalytic activity in a controlled fashion (Figures 4b and

https://dx.doi.org/10.1021/acsami.0c09472
ACS Appl. Mater. Interfaces XXXX, XXX, XXX−XXX

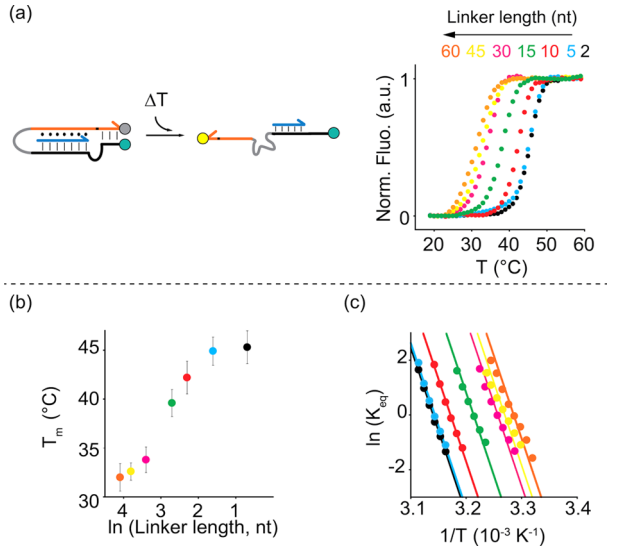

Figure 3. (a,b) Using the DNAzyme variants, we have performed melting curve experiments and (c) obtained van't Hoff plots, by fixing the slope (and thus the enthalpy) as the mean of the different slopes reported in Figure S1, to measure the entropy associated with the linker domain. Melting curve experiments were performed at a concentration of each DNAzyme variant of 20 nM and 5 μM of DNA substrate at a rate of 1 °C·min^{-1}.

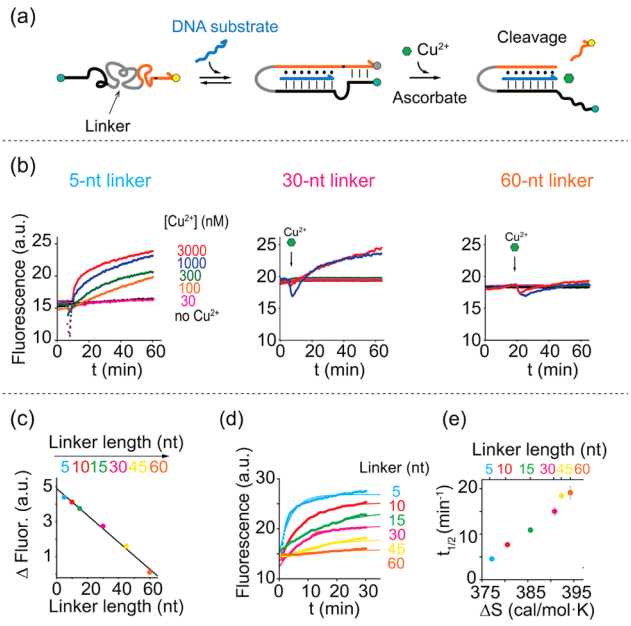

Figure 4. (a) Clamp-like strand forms the catalytic core binding the DNA substrate strand and undergoes self-cleavage activity upon the addition of Cu^{2+} ions. (b) Titration curves obtained at increasing concentrations of Cu^{2+} ions for all the DNAzyme variants. (c) The observed efficiency of the catalytic activity decreases with the length of the linker domain. ΔFluor represents the increase in fluorescence recorded after 30 min from the addition of Cu^{2+} ions. (d) Fluorescent kinetic traces of the cleavage reaction for all the variants observed in the presence of DNA substrate (300 nM) and Cu^{2+} ions (3 μM). (e) Apparent half-time of cleavage reaction values ($t_{1/2}$) obtained by fitting the kinetic traces (panel d) using a single exponential.

S3). Of note, the quick decrease of the fluorescence signal can be ascribed to the Cu^{2+}-induced folding of the DNAzyme triplex complex. As the self-cleavage reaction of the DNAzyme proceeds, we then observe the increase of the fluorescence signal due to the release of the fluorophore from the quencher. Denaturing urea/polyacrylamide gel electrophoresis (UREA PAGE) experiments further support the observation that cleavage only occurs upon the addition of Cu^{2+} ions and with a different efficiency and kinetics for the tested variants (Figure S4). As expected, DNAzymes with longer linker length show a decreased catalytic activity, associated with the higher entropic cost of the linker domain (Figure 4c). A monotonic increment of the half-time of the cleavage reaction increasing the length of the linker domain was observed (Figure 4d,e).

Control experiments employing mismatched DNA substrates (not able to form the triplex structure because of one or three mismatch bases) also provided a demonstration that the catalytic core of the DNAzyme is crucial for the Cu^{2+}-dependent nuclease activity. As expected, in the presence of saturating concentration of Cu^{2+} ions, the cleavage is not observed for all the variants (Figure S5). Moreover, the catalytic capability of the Cu^{2+}-dependent DNAzyme was also tested with a split hairpin (without the linker). Also in this case, no cleavage activity was observed, thus further supporting the role of the linker domain in the functionality of the DNAzyme (Figure S6). Finally, the DNAzyme is highly specific toward Cu^{2+} ions, and no activity was observed in the presence of different nonspecific metal ions (Figure S7).

CONCLUSIONS

We demonstrated here a novel approach to rationally control and modulate the activity of DNAzymes in a predictable and fine way. To do so, we took inspiration from nature, in which the activity of proteins and enzymes is often modulated through changes in the entropy associated with intrinsically disordered portions that are not directly involved in the recognition event. Inspired by this elegant naturally occurring mechanism, we rationally re-engineered here the well-known Cu^{2+}-dependent self-cleaving DNAzyme introducing an intrinsically disordered domain in its sequence. Specifically, we designed a poly(T) linker strand that connects the two functional portions of the DNAzyme that fold into the catalytic core displaying self-cleavage enzyme-like activity. By varying the length of this linker strand and thus the entropy associated with it, we have achieved a fine modulation of the DNAzyme catalytic activity. Because the entropic contribution of a single-stranded DNA sequence can be easily programmed, the recreation of such a mechanism to finely regulate the catalytic activity of DNAzymes and, in analogy, ribozymes,[46] appears advantageous compared to other strategies employed to date. In conclusion, entropy may thus represent a further level of control of DNAzyme catalytic activity for a wide range of different applications, including biosensors and synthetic biology.

ASSOCIATED CONTENT

Supporting Information

The Supporting Information is available free of charge at https://pubs.acs.org/doi/10.1021/acsami.0c09472.

Calculated values of K_D (Table S1), T_m and enthalpy values (Table S2), entropy values (Table S3), van't Hoff plots (Figure S1), entropy values scaled with the natural logarithm of the number of nucleotides in the linker domain (Figure S2), titration curves (Figure S3),

https://dx.doi.org/10.1021/acsami.0c09472
ACS Appl. Mater. Interfaces XXXX, XXX, XXX−XXX

denaturing UREA PAGE gels (Figure S4), specificity tests (Figures S5−S7) (PDF)

AUTHOR INFORMATION

Corresponding Author

Francesco Ricci − *Chemistry Department, University of Rome, Tor Vergata, 00133 Rome, Italy;* orcid.org/0000-0003-4941-8646; Email: francesco.ricci@uniroma2.it

Authors

Daniela Sorrentino − *Chemistry Department, University of Rome, Tor Vergata, 00133 Rome, Italy;* orcid.org/0000-0001-5669-0280

Simona Ranallo − *Chemistry Department, University of Rome, Tor Vergata, 00133 Rome, Italy;* orcid.org/0000-0002-2328-6334

Complete contact information is available at: https://pubs.acs.org/10.1021/acsami.0c09472

Notes

The authors declare no competing financial interest.

ACKNOWLEDGMENTS

This work was supported by Associazione Italiana per la Ricerca sul Cancro, AIRC (project n. 21965) (F.R.), by the European Research Council, ERC (Consolidator Grant project n. 819160) (F.R.), and by the Italian Ministry of University and Research (Project of National Interest, PRIN, n. 2015TWP83Z, 2019) (F.R.). S.R. is supported by European Union's Horizon 2020 research and innovation program under the Marie Skłodowska-Curie grant agreement n. 843179 ("DNA-NANO-AB").

REFERENCES

(1) Breaker, R. R.; Joyce, G. F. The Expanding View of RNA and DNA Function. *Chem. Biol.* **2014**, *21*, 1059−1065.

(2) Kruger, K.; Grabowski, P. J.; Zaug, A. J.; Sands, J.; Gottschling, D. E.; Cech, T. R. Self-splicing RNA: autoexcision and autocyclization of the ribosomal RNA intervening sequence of Tetrahymena. *Cell* **1982**, *31*, 147−157.

(3) Cech, T. R. Self-Splicing and Enzymatic Activity of an Intervening Sequence RNA from Tetrahymena. *Angew. Chem., Int. Ed. Engl.* **1990**, *29*, 759−768.

(4) Altman, S.; Baer, M.; Guerrier-Takada, C.; Vioque, A. Enzymatic Cleavage of RNA by RNA. *Trends Biochem. Sci.* **1986**, *11*, 515−518.

(5) Breaker, R. R.; Joyce, G. F. A DNA Enzyme that Cleaves RNA. *Chem. Biol.* **1994**, *1*, 223−229.

(6) Li, Y.; Breaker, R. R. Phosphorylating DNA with DNA. *Proc. Natl. Acad. Sci. U. S. A.* **1999**, *96*, 2746−2751.

(7) Sreedhara, A.; Li, Y.; Breaker, R. R. Ligating DNA with DNA. *J. Am. Chem. Soc.* **2004**, *126*, 3454−3560.

(8) Sheppard, T. L.; Ordoukhanian, P.; Joyce, G. F. A DNA Enzyme with N-glycosylase Activity. *Proc. Natl. Acad. Sci. U. S. A.* **2000**, *97*, 7802−7807.

(9) Chandra, M.; Sachdeva, A.; Silverman, S. K. DNA-Catalyzed Sequence-Specific Hydrolysis of DNA. *Nat. Chem. Biol.* **2009**, *5*, 718−720.

(10) Zhou, W.; Saran, R.; Liu, J. Metal Sensing by DNA. *Chem. Rev.* **2017**, *117*, 8272−8325.

(11) Carmi, N.; Shultz, L. A.; Breaker, R. R. In Vitro Selection of Self-Cleaving DNAs. *Chem. Biol.* **1996**, *3*, 1039−1046.

(12) Carmi, N.; Balkhi, S. R.; Breaker, R. R. Cleaving DNA with DNA. *Proc. Natl. Acad. Sci. U. S. A.* **1998**, *95*, 2233−2237.

(13) Carmi, N.; Breaker, R. R. Characterization of a DNA-cleaving Deoxyribozyme. *Bioorg. Med. Chem.* **2001**, *9*, 2589−2600.

(14) Liu, J.; Lu, Y. A DNAzyme Catalytic Beacon Sensor for Paramagnetic Cu^{2+} Ions in Aqueous Solution with High Sensitivity and Selectivity. *J. Am. Chem. Soc.* **2007**, *129*, 9838−9839.

(15) Liu, J.; Lu, Y. Accelerated Color Change of Gold Nanoparticles Assembled by DNAzymes for Simple and Fast Colorimetric Pb^{2+} Detection. *J. Am. Chem. Soc.* **2004**, *126*, 12298−12305.

(16) Liu, S.; Cheng, C.; Gong, H.; Wang, L. Programmable Mg^{2+}-dependent DNAzyme Switch by the Catalytic Hairpin DNA Assembly For Dual-Signal Amplification Toward Homogeneous Analysis of Protein and DNA. *Chem. Commun.* **2015**, *51*, 7364−7367.

(17) Gu, H.; Furukawa, K.; Weinberg, Z.; Berenson, D. F.; Breaker, R. R. Small, Highly Active DNAs That Hydrolyze DNA. *J. Am. Chem. Soc.* **2013**, *135*, 9121−9129.

(18) Hollenstein, M.; Hipolito, C.; Lam, C.; Dietrich, D.; Perrin, D. A Highly Selective DNAzyme Sensor for Mercuric Ions. *Angew. Chem., Int. Ed.* **2008**, *47*, 4346−4350.

(19) Li, Y.; Sen, D. A Catalytic DNA for Porphyrin Metallation. *Nat. Struct. Mol. Biol.* **1996**, *3*, 743−747.

(20) Wang, S.; Yue, L.; Shpilt, Z.; Cecconello, A.; Kahn, J. S.; Lehn, J.-M.; Willner, I. Controlling the Catalytic Functions of DNAzymes within Constitutional Dynamic Networks of DNA Nanostructures. *J. Am. Chem. Soc.* **2017**, *139*, 9662−9671.

(21) Wang, F.; Lu, C.-H.; Willner, I. From Cascaded Catalytic Nucleic Acids to Enzyme−DNA Nanostructures: Controlling Reactivity, Sensing, Logic Operations, and Assembly of Complex Structures. *Chem. Rev.* **2014**, *114*, 2881−2941.

(22) Mao, X.; Simon, A. J.; Pei, H.; Shi, J.; Li, J.; Huang, Q.; Plaxco, K. W.; Fan, C. Activity Modulation and Allosteric Control of a Scaffolded DNAzyme Using a Dynamic DNA Nanostructure. *Chem. Sci.* **2016**, *7*, 1200−1204.

(23) Mao, X.; Li, Q.; Zuo, X.; Fan, C. Catalytic Nucleic Acids for Bioanalysis. *ACS Appl. Bio Mater.* **2020**, *3*, 2674−2685.

(24) Chen, F.; Bai, M.; Cao, K.; Zhao, Y.; Cao, X.; Wei, J.; Wu, N.; Li, J.; Wang, L.; Fan, C.; Zhao, Y. Programming Enzyme-Initiated Autonomous DNAzyme Nanodevices in Living Cells. *ACS Nano* **2017**, *11*, 11908−11914.

(25) Wen, Y.; Xu, Y.; Mao, X.; Wei, Y.; Song, H.; Chen, N.; Huang, Q.; Fan, C.; Li, D. DNAzyme-Based Rolling-Circle Amplification DNA Machine for Ultrasensitive Analysis of MicroRNA in Drosophila Larva. *Anal. Chem.* **2012**, *84*, 7664−7669.

(26) Wen, Y.; Peng, C.; Li, D.; Zhuo, L.; He, S.; Wang, L.; Huang, Q.; Xu, Q.-H.; Fan, C. Metal Ion-Modulated Graphene-DNAzyme Interactions: Design of a Nanoprobe for Fluorescent Detection of Lead(II) Ions with High Sensitivity, Selectivity and Tunable Dynamic Range. *Chem. Commun.* **2011**, *47*, 6278−6280.

(27) Wang, D. Y.; Lai, B. H. Y.; Feldman, A. R.; Sen, D. A. A General Approach for the Use of Oligonucleotide Effectors to Regulate the Catalysis of RNA-Cleaving Ribozymes and DNAzymes. *Nucleic Acids Res.* **2002**, *30*, 1735−1742.

(28) Chen, W.-H.; Yu, X.; Cecconello, A.; Sohn, Y. S.; Nechushtai, R.; Willner, I. Stimuli-Responsive Nucleic Acid-Functionalized Metal−Organic Framework Nanoparticles Using pH- and Metal-Ion-Dependent Dnazymes As Locks. *Chem. Sci.* **2017**, *8*, 5769−5780.

(29) Levy, M.; Ellington, A. D. ATP-Dependent Allosteric DNA Enzymes. *Chem. Biol.* **2002**, *9*, 417−426.

(30) Lam, B. J.; Joyce, G. F. Autocatalytic Aptazymes Enable Ligand-Dependent Exponential Amplification of RNA. *Nat. Biotechnol.* **2009**, *27*, 288−292.

(31) Hartig, J. S.; Najafi-Shoushtari, S. H.; Grune, I.; Yan, A.; Ellington, A. D.; Famulok, M. Protein-Dependent Ribozymes Report Molecular Interactions in Real Time. *Nat. Biotechnol.* **2002**, *20*, 717−722.

(32) Teller, C.; Shimron, S.; Willner, I. Aptamer−Dnazyme Hairpins for Amplified Biosensing. *Anal. Chem.* **2009**, *81*, 9114−9119.

(33) Chen, Y.; Song, Y.; He, Z.; Wang, Z.; Liu, W.; Wang, F.; Zhang, X.; Zhou, X. pH-Controlled Dnazymes: Rational Design and their Applications in DNA-Machinery Devices. *Nano Res.* **2016**, *9*, 3084−3092.

https://dx.doi.org/10.1021/acsami.0c09472
ACS Appl. Mater. Interfaces XXXX, XXX, XXX−XXX

(34) Elbaz, J.; Shimron, S.; Willner, I. pH-triggered switchable Mg^{2+}-Dependent DNAzymes. *Chem. Commun.* **2010**, *46*, 1209−1211.
(35) Elbaz, J.; Wang, F.; Remacle, F.; Willner, I. pH-programmable DNA Logic Arrays Powered by Modular DNAzyme Libraries. *Nano Lett.* **2012**, *12*, 6049−6054.
(36) Mariottini, D.; Idili, A.; Nijenhuis, M. A. D.; de Greef, T. F. A.; Ricci, F. DNA-Based Nanodevices Controlled by Purely Entropic Linker Domains. *J. Am. Chem. Soc.* **2018**, *140*, 14725−14734.
(37) Mariottini, D.; Idili, A.; Nijenhuis, M. A. D.; Ercolani, G.; Ricci, F. Entropy-Based Rational Modulation of the pKa of a Synthetic pH-Dependent Nanoswitch. *J. Am. Chem. Soc.* **2019**, *141*, 11367−11371.
(38) Tzeng, S.-R.; Kalodimos, C. G. Protein Activity Regulation by Conformational Entropy. *Nature* **2012**, *488*, 236−240.
(39) Xie, H.; Vucetic, S.; Iakoucheva, L. M.; Oldfield, C. J.; Dunker, A. K.; Uversky, V. N.; Obradovic, Z. J. Functional Anthology of Intrinsic Disorder. Biological Processes and Functions of Proteins with Long Disordered Regions. *Prot. Res.* **2007**, *6*, 1882−1898.
(40) Dunker, A. K.; Brown, C. J.; Lawson, J. D.; Iakoucheva, L. M.; Obradovic, Z. Intrinsic Disorder and Protein Function. *Biochemistry* **2002**, *41*, 6573−6582.
(41) Iakoucheva, L. M.; Radivojac, P.; Brown, C. J.; O'Connor, T. R.; Sikes, J. G.; Obradovic, Z.; Dunker, A. K. The Importance of Intrinsic Disorder for Protein Phosphorylation. *Nucleic Acids Res.* **2004**, *32*, 1037−1049.
(42) Musiani, F.; Ippoliti, E.; Micheletti, C.; Carloni, P.; Ciurli, S. Conformational Fluctuations of UreG, an Intrinsically Disordered Enzyme. *Biochemistry* **2013**, *52*, 2949−2954.
(43) Nussinov, R.; Jang, H.; Tsai, C.-J.; Liao, T.-J.; Li, S.; Fushman, D.; Zhang, J. Intrinsic Protein Disorder in Oncogenic KRAS Signaling. *Cell. Mol. Life Sci.* **2017**, *74*, 3245−3261.
(44) Zadeh, J. N.; Steenberg, C. D.; Bois, J. S.; Wolfe, B. R.; Pierce, M. B.; Khan, A. R.; Dirks, R. M.; Pierce, N. A. NUPACK: Analysis and Design of Nucleic Acid Systems. *J. Comput. Chem.* **2011**, *32*, 170−173.
(45) Mergny, J.-L.; Lacroix, L. Analysis of Thermal Melting Curves. *Oligonucleotides* **2003**, *13*, 515−537.
(46) Ma, L.; Liu, J. Catalytic Nucleic Acids: Biochemistry, Chemical Biology, Biosensors and Nanotechnology. *iScience* **2020**, *23*, 100815.

https://dx.doi.org/10.1021/acsami.0c09472
ACS Appl. Mater. Interfaces XXXX, XXX, XXX−XXX